

Measurement of Parton Distributions of Strange Quarks in the Nucleon from Charged-Kaon Production in Deep-Inelastic Scattering on the Deuteron

A. Airapetian,¹⁶ N. Akopov,²⁷ Z. Akopov,²⁷ A. Andrus,¹⁵ E.C. Aschenauer,⁷ W. Augustyniak,²⁶ R. Avakian,²⁷ A. Avetissian,²⁷ E. Avetissian,¹¹ S. Belostotski,¹⁹ N. Bianchi,¹¹ H.P. Blok,^{18,25} H. Böttcher,⁷ C. Bonomo,¹⁰ A. Borissov,¹⁴ A. Brüll*, V. Bryzgalov,²⁰ J. Burns,¹⁴ M. Capiluppi,¹⁰ G.P. Capitani,¹¹ E. Cisbani,²² G. Ciullo,¹⁰ M. Contalbrigo,¹⁰ P.F. Dalpiaz,¹⁰ W. Deconinck,¹⁶ R. De Leo,² M. Demey,¹⁸ L. De Nardo,^{6,23} E. De Sanctis,¹¹ M. Diefenthaler,⁹ P. Di Nezza,¹¹ J. Dreschler,¹⁸ M. Düren,¹³ M. Ehrenfried,¹³ A. Elalaoui-Moulay,¹ G. Elbakian,²⁷ F. Ellinghaus,⁵ U. Elschenbroich,¹² R. Fabbri,⁷ A. Fantoni,¹¹ L. Felawka,²³ S. Frullani,²² A. Funel,¹¹ D. Gabbert,⁷ G. Gapienko,²⁰ V. Gapienko,²⁰ F. Garibaldi,²² G. Gavrilo, ^{6,19,23} V. Gharibyan,²⁷ F. Giordano,¹⁰ S. Gliske,¹⁶ I.M. Gregor,⁷ H. Guler,⁷ C. Hadjidakis,¹¹ D. Hasch,¹¹ T. Hasegawa,²⁴ W.H.A. Hesselink,^{18,25} G. Hill,¹⁴ A. Hillenbrand,⁹ M. Hoek,¹⁴ Y. Holler,⁶ B. Hommez,¹² I. Hristova,⁷ G. Iarygin,⁸ Y. Imazu,²⁴ A. Ivanilov,²⁰ A. Izotov,¹⁹ H.E. Jackson,¹ A. Jgoun,¹⁹ S. Joosten,¹² R. Kaiser,¹⁴ T. Keri,¹³ E. Kinney,⁵ A. Kisselev,^{15,19} T. Kobayashi,²⁴ M. Kopytin,⁷ V. Korotkov,²⁰ V. Kozlov,¹⁷ P. Kravchenko,¹⁹ V.G. Krivokhijine,⁸ L. Lagamba,² R. Lamb,¹⁵ L. Lapikás,¹⁸ I. Lehmann,¹⁴ P. Lenisa,¹⁰ P. Liebing,⁷ L.A. Linden-Levy,¹⁵ A. Lopez Ruiz,¹² W. Lorenzon,¹⁶ S. Lu,¹³ X.-R. Lu,²⁴ B.-Q. Ma,³ D. Mahon,¹⁴ B. Maiheu,¹² N.C.R. Makins,¹⁵ L. Manfré,²² Y. Mao,³ B. Marianski,²⁶ H. Marukyan,²⁷ V. Mexner,¹⁸ C.A. Miller,²³ Y. Miyachi,²⁴ V. Muccifora,¹¹ M. Murray,¹⁴ A. Mussgiller,⁹ A. Nagaitsev,⁸ E. Nappi,² Y. Naryshkin,¹⁹ A. Nass,⁹ M. Negodaev,⁷ W.-D. Nowak,⁷ A. Osborne,¹⁴ L.L. Pappalardo,¹⁰ R. Perez-Benito,¹³ N. Pickert,⁹ M. Raithel,⁹ D. Reggiani,⁹ P.E. Reimer,¹ A. Reischl,¹⁸ A.R. Reolon,¹¹ C. Riedl,¹¹ K. Rith,⁹ S.E. Rock,⁶ G. Rosner,¹⁴ A. Rostomyan,⁶ L. Rubacek,¹³ J. Rubin,¹⁵ D. Ryckbosch,¹² Y. Salomatin,²⁰ I. Sanjiev,^{1,19} A. Schäfer,²¹ G. Schnell,¹² K.P. Schüller,⁶ B. Seitz,¹⁴ C. Shearer,¹⁴ T.-A. Shibata,²⁴ V. Shutov,⁸ M. Stancari,¹⁰ M. Statera,¹⁰ E. Steffens,⁹ J.J.M. Steijger,¹⁸ H. Stenzel,¹³ J. Stewart,⁷ F. Stinzinger,⁹ J. Streit,¹³ P. Tait,⁹ S. Taroian,²⁷ B. Tchuiko,²⁰ A. Terkulov,¹⁷ A. Trzcinski,²⁶ M. Tytgat,¹² A. Vandenbroucke,¹² P.B. van der Nat,¹⁸ G. van der Steenhoven,¹⁸ Y. van Haarlem,¹² C. van Hulse,¹² M. Varanda,⁶ D. Veretennikov,¹⁹ V. Vikhrov,¹⁹ I. Vilardi,² C. Vogel,⁹ S. Wang,³ S. Yaschenko,⁹ H. Ye,³ Y. Ye,⁴ Z. Ye,⁶ S. Yen,²³ W. Yu,¹³ D. Zeiler,⁹ B. Zihlmann,¹² and P. Zupranski²⁶

(The HERMES Collaboration)

¹Physics Division, Argonne National Laboratory, Argonne, Illinois 60439-4843, USA

²Istituto Nazionale di Fisica Nucleare, Sezione di Bari, 70124 Bari, Italy

³School of Physics, Peking University, Beijing 100871, China

⁴Department of Modern Physics, University of Science and Technology of China, Hefei, Anhui 230026, China

⁵Nuclear Physics Laboratory, University of Colorado, Boulder, Colorado 80309-0390, USA

⁶DESY, 22603 Hamburg, Germany

⁷DESY, 15738 Zeuthen, Germany

⁸Joint Institute for Nuclear Research, 141980 Dubna, Russia

⁹Physikalisches Institut, Universität Erlangen-Nürnberg, 91058 Erlangen, Germany

¹⁰Istituto Nazionale di Fisica Nucleare, Sezione di Ferrara and

Dipartimento di Fisica, Università di Ferrara, 44100 Ferrara, Italy

¹¹Istituto Nazionale di Fisica Nucleare, Laboratori Nazionali di Frascati, 00044 Frascati, Italy

¹²Department of Subatomic and Radiation Physics, University of Gent, 9000 Gent, Belgium

¹³Physikalisches Institut, Universität Gießen, 35392 Gießen, Germany

¹⁴Department of Physics and Astronomy, University of Glasgow, Glasgow G12 8QQ, United Kingdom

¹⁵Department of Physics, University of Illinois, Urbana, Illinois 61801-3080, USA

¹⁶Randall Laboratory of Physics, University of Michigan, Ann Arbor, Michigan 48109-1040, USA

¹⁷Lebedev Physical Institute, 117924 Moscow, Russia

¹⁸Nationaal Instituut voor Kernfysica en Hoge-Energiefysica (NIKHEF), 1009 DB Amsterdam, The Netherlands

¹⁹Petersburg Nuclear Physics Institute, St. Petersburg, Gatchina, 188350 Russia

²⁰Institute for High Energy Physics, Protvino, Moscow region, 142281 Russia

²¹Institut für Theoretische Physik, Universität Regensburg, 93040 Regensburg, Germany

²²Istituto Nazionale di Fisica Nucleare, Sezione Roma 1, Gruppo Sanità and Physics Laboratory, Istituto Superiore di Sanità, 00161 Roma, Italy

²³TRIUMF, Vancouver, British Columbia V6T 2A3, Canada

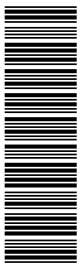
²⁴Department of Physics, Tokyo Institute of Technology, Tokyo 152, Japan

²⁵Department of Physics and Astronomy, Vrije Universiteit, 1081 HV Amsterdam, The Netherlands

²⁶Andrzej Soltan Institute for Nuclear Studies, 00-689 Warsaw, Poland

²⁷Yerevan Physics Institute, 375036 Yerevan, Armenia

(Dated: June 4, 2008)



The momentum and helicity density distributions of the strange quark sea in the nucleon are obtained in leading order from charged-kaon production in deep-inelastic scattering on the deuteron. The distributions are extracted from spin-averaged K^\pm multiplicities, and from K^\pm and inclusive double-spin asymmetries for scattering of polarized positrons by a polarized deuterium target. The shape of the momentum distribution is softer than that of the average of the \bar{u} and \bar{d} quarks. In the region of measurement $0.02 < x < 0.6$ and $Q^2 > 1.0 \text{ GeV}^2$, the helicity distribution is zero within experimental uncertainties.

PACS numbers: 13.60.-r, 13.88.+e, 14.20.Dh, 14.65.-q

Parton distribution functions (PDFs) form the basis for the description of the flavor structure of the nucleon. The spin-averaged parton distribution functions $q(x)$ of quarks and antiquarks of flavors $q = (u, d, s)$ [1, 2] describe the quark momentum contributions, where x is the dimensionless Bjorken scaling variable representing the momentum fraction of the target carried by the parton in a frame where the target has “infinite” longitudinal momentum. They are sums of the number densities of the quarks $q_{\rightarrow}(x)$ [$q_{\leftarrow}(x)$] with the same [opposite] helicity as that of the nucleon. The differences, or helicity distributions, $\Delta q(x) = q_{\rightarrow}(x) - q_{\leftarrow}(x)$ describe the flavor dependent contributions of the quark spins to the spin of the nucleon. The features of the parton distributions reflect the QCD dynamics of the constituents. Because strange quarks are objects which reflect directly properties of the nucleon sea, they are of special interest. Their distributions are also important because of their impact on quantitative calculations of certain key short-distance processes at hadron colliders, and their implications for the measurement of the Weinberg angle in deep-inelastic scattering (DIS) of neutrinos [3, 4].

In the absence of significant experimental constraints, current global QCD fits of PDFs [5, 6] assume the strange quark and antiquark momentum distributions $s(x)$ and $\bar{s}(x)$ to be given by $s(x) = \bar{s}(x) = r[\bar{u}(x) + \bar{d}(x)]/2$ with $r \approx 1/2$ at some low factorization scale. Measurements of neutrino and antineutrino production of dimuons [7, 8, 9, 10, 11, 12, 13, 14, 15] provide useful but limited information [16] on the normalization and shape of the distribution $s(x) + \bar{s}(x)$. In these experiments, extraction of the strange quark distributions requires knowledge of the charm quark mass, the charm hadron semileptonic branching ratio, and the “Peterson fragmentation parameter” [17] that describes the kinematic dependence of the charm fragmentation function. These quantities together with the strange parton distributions themselves are fitted simultaneously in the extraction procedure. Much of the information on properties of the helicity distribution of strange quarks is based on the analysis of inclusive DIS and hyperon decay under the assumption of SU(3) symmetry among the structures

of the octet baryons. In these inclusive experiments [18] the first moment of the helicity distribution for strange quarks is one of the principal results. The most precise recent value is $-0.103 \pm 0.007(\text{exp.}) \pm 0.013(\text{theor.}) \pm 0.008(\text{evol.})$ in LO [19]. A full 5-flavor decomposition using HERMES semi-inclusive DIS [20] data from proton and deuteron targets, although not sensitive to $\Delta\bar{s}(x)$, yielded $\Delta s = 0.028 \pm 0.033 \pm 0.009$ for the first partial moment of the strange quark helicity density in the measured range $0.023 < x < 0.3$. A separate “isoscalar” extraction of $\Delta s + \Delta\bar{s}$ from DIS data on the deuteron alone gave $\Delta s + \Delta\bar{s} = 0.129 \pm 0.042 \pm 0.129$ in the measured range where the large systematic uncertainty reflected lack of knowledge of kaon fragmentation functions.

This letter reports a new isoscalar extraction of $s(x) + \bar{s}(x)$ and $\Delta(s(x) + \bar{s}(x))$ based on the same HERMES data obtained from polarized DIS on a deuterium target. The measurement reported here is complementary to the neutrino results, and is the first extraction of $s(x) + \bar{s}(x)$ in charged lepton DIS. Because strange quarks carry no isospin, the strange seas in the proton and neutron can be assumed to be identical. In the deuteron, an isoscalar target, the fragmentation process in DIS can be described by fragmentation functions that have no isospin dependence. Aside from isospin symmetry between proton and neutron, the only symmetry assumed is charge-conjugation invariance in fragmentation. For the isoscalar deuteron in Leading Order (LO), the inclusive unpolarized (U) electron scattering cross section in terms of the parton distributions $Q(x) \equiv u(x) + \bar{u}(x) + d(x) + \bar{d}(x)$ and $S(x) \equiv s(x) + \bar{s}(x)$ takes the form

$$\frac{d^2 N^{DIS}(x)}{dx dQ^2} = \mathcal{K}_U(x, Q^2) [5Q(x) + 2S(x)], \quad (1)$$

where $\mathcal{K}_U(x, Q^2)$ is a kinematic factor containing the hard scattering cross section. The weak logarithmic dependence of the PDFs on $-Q^2$, the squared four-momentum of the exchanged virtual photon, has been suppressed for simplicity. Applying the same LO formalism to the semi-inclusive cross section for charged kaon production, irrespective of charge, hereafter designated as K gives

$$\frac{d^2 N^K(x)}{dx dQ^2} = \mathcal{K}_U(x, Q^2) \times \left[Q(x) \int \mathcal{D}_Q^K(z) dz + S(x) \int \mathcal{D}_S^K(z) dz \right], \quad (2)$$

*Present address: Thomas Jefferson National Accelerator Facility, Newport News, Virginia 23606, USA

where $z \equiv E_h/\nu$ with ν and E_h the energies of the virtual photon and of the detected hadron in the target rest frame, $\mathcal{D}_Q^K(z) \equiv 4D_u^K(z) + D_d^K(z)$ and $\mathcal{D}_S^K(z) \equiv 2D_s^K(z)$. The fragmentation function $\mathcal{D}_q^K(z)$ describing the number density of charged kaons from a struck quark of flavor q is integrated over the measured range of z . Combining Eqs. (1,2) and neglecting the term $2S(x)$ compared to $5Q(x)$, it follows immediately that

$$S(x) \int \mathcal{D}_S^K(z) dz \simeq Q(x) \left[5 \frac{d^2 N^K(x)}{d^2 N^{DIS}(x)} - \int \mathcal{D}_Q^K(z) dz \right]. \quad (3)$$

Eq. 3 is the basis for the extraction of the quantity $S(x) \int \mathcal{D}_S^K(z) dz$.

The data were recorded with a longitudinally nuclear-polarized deuteron gas target internal to the $E = 27.6$ GeV HERA positron storage ring at DESY. The self-induced beam polarization was measured continuously with Compton backscattering of circularly polarized laser beams [21, 22]. The open-ended target cell was fed by an atomic-beam source based on Stern-Gerlach separation with hyperfine transitions. The nuclear polarization of the atoms was flipped at 90s time intervals, while both this polarization and the atomic fraction inside the target cell were continuously measured [23]. The average value of the deuteron polarization was 0.845 with a fractional systematic uncertainty of 3.5%.

Scattered beam leptons and coincident hadrons were detected by the HERMES spectrometer [24]. Leptons were identified with an efficiency exceeding 98% and a hadron contamination of less than 1% using an electromagnetic calorimeter, a transition-radiation detector, a preshower scintillation counter and a ring-imaging Čerenkov (RICH) detector [25]. The dual-radiator RICH was also used to identify charged kaons. Events were selected subject to the kinematic requirements $Q^2 > 1 \text{ GeV}^2$, $W^2 > 10 \text{ GeV}^2$ and $y < 0.85$, where W is the invariant mass of the photon-nucleon system, and $y = \nu/E$. Coincident hadrons were accepted if $0.2 < z < 0.8$ and $x_F \approx 2p_L/W > 0.1$, where p_L is the longitudinal momentum of the hadron with respect to the virtual photon direction in the photon-nucleon center of mass frame. The Bjorken x range of measurement was 0.02–0.6.

The charged kaon multiplicity was extracted by summing over the kaon yields for the two beam-target polarization states. An event weighting procedure was used to correct for RICH kaon identification inefficiencies. The effects of QED radiation, instrumental resolution, and acceptance were simulated [26, 27, 28], and corrections were applied to the data for each polarization state using a technique that unfolds kinematic migration of events [19]. The results are presented in Fig. 1. The trends in the data were not reproduced (see dotted curve in Fig. 1) by fitting the points using the CTEQ6L [29] strange quark PDFs in Eqs. 1 and 2, with $\int \mathcal{D}_Q^K(z) dz$

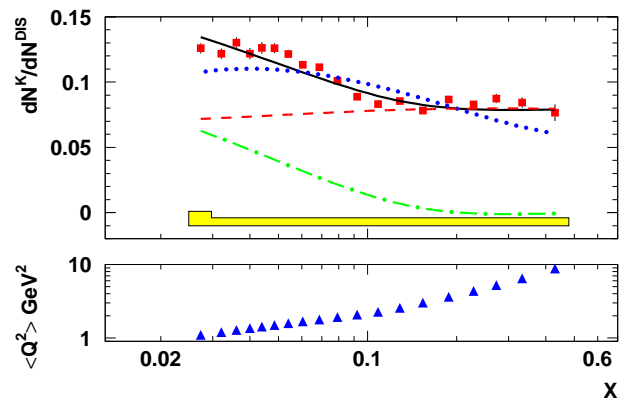


FIG. 1: The multiplicity corrected to 4π of charged kaons in semi-inclusive DIS from a deuterium target, as a function of Bjorken x . The continuous curve is calculated from the curve in Fig. 2 using Eq. 3. The dashed(dash-dotted) curve is the nonstrange(strange) quark contribution to the multiplicity for this fit. The dotted curve is the best fit to $\int \mathcal{D}_S^K(z) dz$ using CTEQ6L PDFs. The error bars are statistical. The band represents the systematic uncertainties. The values of $\langle Q^2 \rangle$ for each x bin are shown in the lower panel.

and $\int \mathcal{D}_S^K(z) dz$ as free parameters. In view of the paucity of reliable data on $S(x)$, it was assumed instead that it is unknown, and the analysis was carried out extracting the product $S(x) \int \mathcal{D}_S^K(z) dz$ in LO. For $x > 0.15$ the multiplicity is constant at a value of about 0.080, implying that $S(x)/Q(x)$ is constant. For this analysis $S(x)$ is assumed to be negligible at large x from which it follows that $S(x) = 0$ for $x > 0.15$ and that $\int_{0.2}^{0.8} \mathcal{D}_Q^K(z) dz = 0.398 \pm 0.010$, in excellent agreement with the value 0.435 ± 0.044 obtained for $Q^2 = 2.5 \text{ GeV}^2$ from the most recent global analysis of fragmentation functions [30]. The value 0.398 was then used in Eq. (3) together with values of $Q(x)$ from CTEQ6L and the measured multiplicities to obtain the product $S(x) \int \mathcal{D}_S^K(z) dz$ shown in Fig. 2. A small iterative correction was made to account for the neglect of the $2S(x)$ term in Eq. 1.

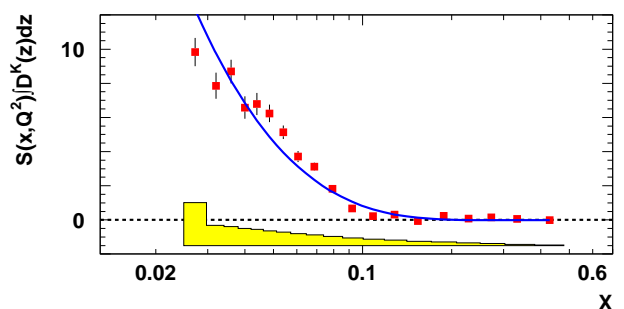


FIG. 2: The strange fragmentation product $S(x, Q^2) \int \mathcal{D}_S^K(z) dz$ obtained from the measured HERMES multiplicity for charged kaons at the $\langle Q^2 \rangle$ for each bin. The curve is a least squares fit of the form $x^{-0.863} e^{-x/0.0487} (1-x)$. The band represents systematic uncertainties.

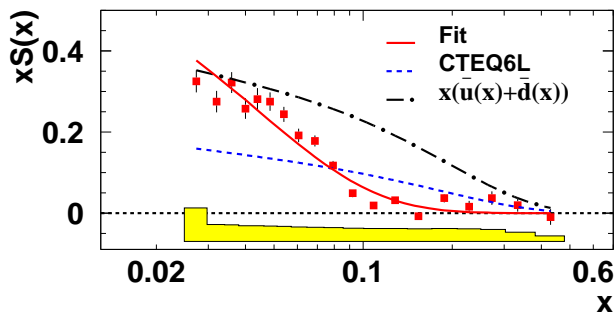


FIG. 3: The strange parton distribution $xS(x)$ from the measured HERMES multiplicity for charged kaons evolved to $Q_0^2 = 2.5 \text{ GeV}^2$ assuming $\int \mathcal{D}_S^K(z) dz = 1.27 \pm 0.13$. The solid curve is a 3-parameter fit for $S(x) = x^{-0.924} e^{-x/0.0404} (1-x)$, the dashed curve gives $xS(x)$ from CTEQ6L, and the dot-dash curve is the sum of light antiquarks from CTEQ6L.

The result for the product together with a fit of the form $x^{-a_1} e^{-x/a_2} (1-x)$ is shown in Fig. 2, and leads to the continuous curve in Fig. 1.

The improved fit (continuous curve in Fig. 1) to the multiplicity is an indication that the actual distribution of $S(x)$ is substantially different from the average of those of the nonstrange antiquarks. To explore this point, the HERMES result for $S(x) \int \mathcal{D}_S^K(z) dz$ has been evolved to $Q_0^2 = 2.5 \text{ GeV}^2$. The Q^2 evolution factors were taken from CTEQ6L and the fragmentation function compilation given in [30]. Consideration of corrections to the evolution due to higher twist contributions is not necessary, since higher twist effects are expected to be significant [31] only for larger values of x where the extracted distribution of $xS(x)$ vanishes. The distribution of $xS(x)$ was obtained from $S(x) \int \mathcal{D}_S^K(z) dz$ by dividing by $\int \mathcal{D}_S^K(z) dz = 1.27 \pm 0.13$, the value at $Q^2 = 2.5 \text{ GeV}^2$ given in [30]. The results are presented in Fig. 3. The normalization of the HERMES points is determined by the value of $\int \mathcal{D}_S^K(z) dz$ assumed. However, whatever the normalization, the shape of $xS(x)$ implied by the HERMES data is incompatible with $xS(x)$ from CTEQ6L as well as the assumption of an average of an isoscalar nonstrange sea. The absence of strength above $x \approx 0.1$ is clearly discrepant with CTEQ6L, while deviations from the CTEQ6L prediction at low x could be, in part, a manifestation of higher order processes.

In the isoscalar extraction of the helicity distribution $\Delta S(x) = \Delta s(x) + \Delta \bar{s}(x)$, only the double-spin asymmetry $A_{\parallel,d}^{K^\pm}(x, Q^2)$ for all charged kaons, irrespective of charge, and the inclusive asymmetry $A_{\parallel,d}(x, Q^2)$ are used. In LO, the inclusive and the charged kaon double-spin(LL) asymmetries are determined by the relations

$$A_{\parallel,d}(x) \frac{d^2 N^{DIS}(x)}{dx dQ^2} = \mathcal{K}_{LL}(x, Q^2) [5\Delta Q(x) + 2\Delta S(x)], \quad (4)$$

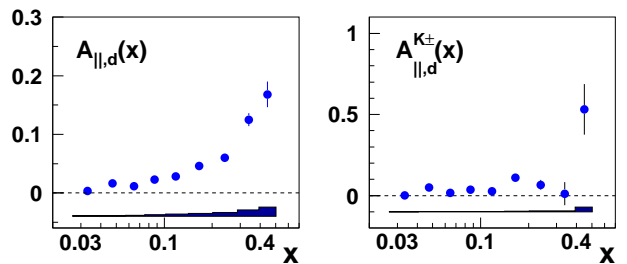


FIG. 4: Lepton-nucleon polarized cross section asymmetries $A_{\parallel,d}$ for inclusive DIS and $A_{\parallel,d}^{K^\pm}$ for semi-inclusive DIS by a deuteron target as a function of Bjorken x , for identified charged kaons. The error bars are statistical, and the bands at the bottom represent the systematic uncertainties.

where \mathcal{K}_{LL} is a kinematic factor, and

$$A_{\parallel,d}^{K^\pm}(x) \frac{d^2 N^K(x)}{dx dQ^2} = \mathcal{K}_{LL}(x, Q^2) \times \left[\Delta Q(x) \int \mathcal{D}_Q^K(z) dz + \Delta S(x) \int \mathcal{D}_S^K(z) dz \right]. \quad (5)$$

Eqs. (4,5) permit the simultaneous extraction of the helicity distribution $\Delta Q(x) = \Delta u(x) + \Delta \bar{u}(x) + \Delta d(x) + \Delta \bar{d}(x)$ and the strange helicity distribution $\Delta S(x) = \Delta s(x) + \Delta \bar{s}(x)$. The nonstrange integrated fragmentation function needed for a LO extraction of $\Delta S(x)$ was extracted from the multiplicity analysis of the same data.

The semi-inclusive asymmetries $A_{\parallel,d}^{K^\pm}$ were derived from the kaon spectra measured for each target polarization. The target polarization was corrected for the D-wave admixture in the deuteron wave function by applying the correction term $(1 - 1.5\omega_D)$ where $\omega = 0.05 \pm 0.01$ [32]. The corrected asymmetries are shown in Fig. 4. The inclusive asymmetries $A_{\parallel,d}(x)$ were corrected for effects of QED radiation and instrumental smearing with the same procedures described above for the spin dependent kaon multiplicities. Contributions to the systematic uncertainties in the asymmetries include those from the beam and target polarizations, and the neglect of the transverse spin structure function $g_2(x) \approx 0$ [33], and for $A_{\parallel,d}^{K^\pm}$ from those of RICH kaon identification.

The quark helicity distributions were extracted from the measured spin asymmetries $A_{\parallel,d}(x)$ and $A_{\parallel,d}^{K^\pm}(x)$ in an analysis based on Eqs. (4,5). The value of $\int \mathcal{D}_S^K(z) dz = 1.27 \pm 0.13$ was used to extract $\Delta S(x)$. The results are presented in Fig. 5. The strange helicity distribution also agrees well with the less precise results of [20], and is consistent with zero over the measured range.

The first moments of the helicity densities in the measured region are presented in Tab. I. The result for ΔQ over the measured range is consistent with the value $0.381 \pm 0.010(\text{stat.}) \pm 0.027(\text{sys.})$ for the full moment previously extracted from HERMES $g_{1,d}$ data [19]. The value of ΔS measured here is not in serious disagreement with $-0.0435 \pm 0.010(\text{stat.}) \pm 0.004(\text{sys.})$ ex-

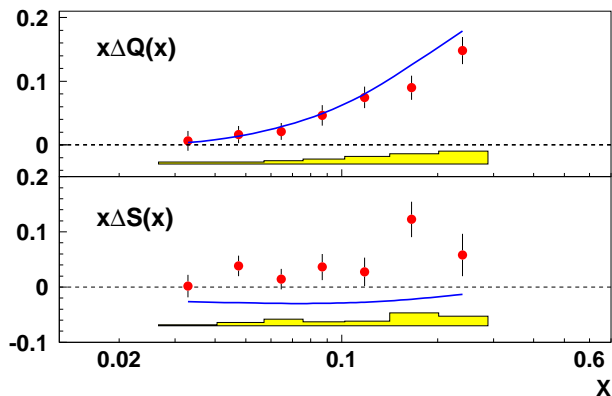


FIG. 5: Nonstrange and strange quark helicity distributions at $Q_0^2 = 2.5 \text{ GeV}^2$, as a function of Bjorken x . The error bars are statistical, and the bands at the bottom represent the systematic uncertainties. The curves are the LO results of Leader *et al.*[38] from their analysis of world data.

tracted from the inclusive HERMES measurements. The value for the partial moment of the octet combination $\Delta q_8(x) = \Delta Q(x) - 2\Delta S(x)$, included in Tab. I, is substantially less than the value of the axial charge $a_8 \equiv \Delta q_8 = \int_0^1 \Delta q_8(x) dx = 0.586 \pm 0.031$ extracted from the hyperon decay constants by assuming SU(3) symmetry [34]. Possible explanations for the deficit observed for Δq_8 include violation of SU(3) symmetry or missing octet strength at values of x below the measured range. The substantial deviation observed in the shape of $S(x)$ from that of the light sea quarks is a clear manifestation of violation of SU(3) symmetry [35, 36, 37] in the strange quark sector.

In conclusion, inclusive and semi-inclusive-charged-kaon spin asymmetries for a longitudinally polarized deuteron target have been analyzed to extract the LO parton distributions of the strange sea in the proton. The partial moment of the nonstrange fragmentation function needed for the LO analysis has been extracted directly from the same data. The values for the PDFs presented in this paper are available at the HERMES web site (<http://www-hermes.desy.de>). The momentum densities are softer than previously assumed. The helicity densities are consistent with zero and the partial moment of the octet axial combination is observed to be substantially less than the axial charge extracted from hyperon decays under the assumption of SU(3) symmetry.

TABLE I: First moments of various helicity distributions in the Bjorken x range 0.02–0.6 at a scale of $Q_0^2 = 2.5 \text{ GeV}^2$.

	Moments in measured range
ΔQ	$0.359 \pm 0.026(\text{stat.}) \pm 0.018(\text{sys.})$
ΔS	$0.037 \pm 0.019(\text{stat.}) \pm 0.027(\text{sys.})$
Δq_8	$0.285 \pm 0.046(\text{stat.}) \pm 0.057(\text{sys.})$

We gratefully acknowledge the DESY management for its support, the staff at DESY and the collaborating institutions for their significant effort, and our national funding agencies for their financial support. We thank D. de Florian, R. Sassot, and M. Stratmann for discussions and the early use of their programs for calculating PDFs and fragmentation functions.

-
- [1] H. L. Lai et al., *Eur. Phys. J. C* **12**, 375 (2000).
 - [2] A. D. Martin et al., *Eur. Phys. J. C* **23**, 73 (2002).
 - [3] F. Olness et al., *Eur. Phys. J. C* **40**, 145 (1998).
 - [4] G. P. Zeller et al. (NuTeV), *Phys. Rev. Lett.* **88**, 091802 (2002).
 - [5] S. Kretzer et al., *Phys. Rev. D* **69**, 114005 (2004).
 - [6] R. S. Thorne et al. (2007), hep-ph/0706.0456.
 - [7] H. Abramowicz et al. (CDHS), *Z. Phys.* **C15**, 19 (1982).
 - [8] S. A. Rabinowitz et al. (CCFR), *Phys. Rev. Lett.* **70**, 134 (1993).
 - [9] A. O. Bazarko et al. (CCFR), *Z. Phys.* **C65**, 189 (1995).
 - [10] P. Vilain et al. (CHARM), *Eur. Phys. J.* **C11**, 19 (1999).
 - [11] P. Astier et al. (NOMAD), *Phys. Lett.* **B486**, 35 (2000).
 - [12] M. Tzanov et al. (NuTeV), *Phys. Rev. D* **74**, 012008 (2006).
 - [13] G. Gerbier et al. (BEBC), *Z. Phys.* **C29**, 15 (1985).
 - [14] N. Ushida et al. (E531), *Phys. Lett.* **B121**, 292 (1983).
 - [15] A. Kayis-Topalsu et al. (CHORUS), *Phys. Lett.* **B626**, 24 (2005).
 - [16] H. L. Lai et al., *J. High Energy Phys.* **4**, 89 (2007).
 - [17] C. Peterson et al., *Phys. Rev. D* **D27**, 105 (1983).
 - [18] J. Ashman et al. (EMC), *Phys. Lett.* **B206**, 364 (1988).
 - [19] A. Airapetian et al. (HERMES), *Phys. Rev. D* **75**, 012007 (2007).
 - [20] A. Airapetian et al. (HERMES), *Phys. Rev. D* **71**, 012003 (2005).
 - [21] D. P. Barber et al., *Nucl. Inst. & Meth.* **A 338**, 166 (1994).
 - [22] M. Beckmann et al., *Nucl. Inst. & Meth.* **A 479**, 334 (2002).
 - [23] A. Airapetian et al., *Nucl. Inst. & Meth.* **A 540**, 68 (2005).
 - [24] K. Ackerstaff et al. (HERMES), *Nucl. Inst. & Meth.* **A 417**, 230 (1998).
 - [25] N. Akopov et al., *Nucl. Inst. & Meth.* **A 479**, 511 (2002).
 - [26] L. Mankiewicz et al., *Comp. Phys. Comm.* **71**, 305 (1992).
 - [27] I. Akushevich et al. (1998), hep-ph/9906408.
 - [28] T. Sjöstrand et al., *Comp. Phys. Comm.* **135**, 238 (2001).
 - [29] J. Pumplin et al., *J. High Energy Phys.* **7**, 12 (2002).
 - [30] D. de Florian et al., *Phys. Rev. D* **75**, 114010 (2007).
 - [31] A. D. Martin et al., *Phys. Lett.* **B443**, 301 (1998).
 - [32] R. Machleidt et al., *Phys. Rep.* **149**, 1 (1987).
 - [33] P. L. Anthony et al. (E155), *Phys. Lett.* **B553**, 18 (2003).
 - [34] P. Ratchliffe, *Czech J. Phys.* **54**, B11 (2004).
 - [35] J. Lichtenstadt and H. J. Lipkin, *Phys. Lett.* **B353**, 119 (1995).
 - [36] E. Leader et al., *Phys. Lett.* **B488**, 283 (2000).
 - [37] O. Schröder et al., *Phys. Lett.* **B439**, 398 (1998).
 - [38] E. Leader et al., *Phys. Rev. D* **73**, 034023 (2006).